Chalcogenide Letters Vol. 19, No. 4, April 2022, p. 285 - 299

High-temperature oxidation resistance of NiCrAlY columnar microcrystalline coating deposited by EDS

R. Y. Wang*, X. L. Feng, C. Yang, R. Wang, C. A. Guo, J. Zhang
Shenyang Ligong University, School of Equipment Engineering, no. 6 Nanping Central Road, Hunnan New District, Shenyang 110159, Liaoning, China

In this paper, the NiCrAlY coating is deposited on the surface of the NiCrAlY alloy substrate by the electrospark deposition method. The phase composition, morphology and element composition of the substrate and coating were characterized by XRD, SEM/EDS. The high-temperature oxidation resistance was tested. The results show that the weight gain of the coating is lower than that of the substrate alloy after high-temperature oxidation. The coating protects the substrate to some extent. And because of the formation of NiCrAlY columnar microcrystalline coating, rich grain boundaries, promoted the diffusion rate of metal ions, resulting in the formation of "pinning effect" of the film/metal interface, improve the anti-stripping performance of the coating.

(Received November 19, 2021; Accepted January 10, 2022)
Keywords: NiCrAlY, High-temperature oxidation, Electrospark deposition, Pinning effect

1. Introduction

In recent years, with the continuous development of industrial technology, the working temperature demand of large industrial equipment gas turbine engine is also increasing to improve the efficiency of equipment. Therefore, higher requirements are put forward for the materials for manufacturing engine parts. Especially hot end turbine components working in harsh environments. At present, the blades of gas turbine engines usually use advanced Nickel-based alloy materials, but these materials are still not durable enough. In order to improve their durability, appropriate coating can protect them from thermal corrosion and high-temperature oxidation. At present, the common method is to coat a protective coating on the surface of components.

Among the existing high temperature protective coatings, NiCrAlY is particularly attractive due to its good adhesion and high-temperature oxidation resistance. It can form a stable protective alumina layer, and its unique composition design can meet specific performance requirements [1-3]. The NiCrAlY coating can promote the formation of Al_2O_3 oxide film with slow growth, uniformity and strong adhesion at service temperature, which acts as a diffusion barrier layer at service temperature [4]. A large number of studies have shown that the oxidation resistance of Ni-rich MCrAlY alloy is better than that of Co-rich MCrAlY alloy under high-temperature oxidation environment. Cr oxides can not only form Cr_2O_3 protective film, but also play a role of "third element" to accelerate the rapid formation of Al_2O_3. The typical MCrAlY

* Corresponding author: 2366599809@qq.com
https://doi.org/10.15251/CL.2022.194.285

coating contains Cr 18-22 *wt.%*, Al 8-12 *wt.%* and Y up to 0.5 *wt.%*. A small amount of active element Y can improve the adhesion of the oxide film [5]. At present, a series of coating deposition processes have been applied to the deposition of NiCrAlY coatings, such as plasma spraying [6], magnetron sputtering [7], and high-speed oxygen gas spraying [8], etc. The above coating preparation methods have been widely used, but the application of electrospark deposition method in the deposition of NiCrAlY alloy is still less. Therefore, in this paper, NiCrAlY coating is deposited on NiCrAlY alloy substrate by electrospark deposition method. The main advantages of using electrospark deposition technology are: The coating deposited by electrospark deposition is metallurgically combined with the substrate, there is no gap between them, and the coating is not easy to peel off [9]. Through research, it is found that the peeling resistance of the coating is more significant than the simple oxidation resistance of the coating [10]. Moreover, due to the rapid cooling in the deposition process of EDS, columnar microcrystalline coating with small grain size can be obtained. The formation of microcrystalline coating can not only enhance the adhesion of the coating, but also quickly form an alumina coating with strong adhesion, slow growth, thermodynamic stability and continuity on the surface of the coating in the process of high-temperature oxidation, It can effectively improve the high-temperature oxidation resistance of the coating.

In this paper, NiCrAlY coating was deposited on the surface of NiCrAlY alloy by EDS, and the element composition and phase composition of substrate and coating were tested by SEM/ESD, XRD. The high-temperature oxidation resistance of coating and substrate was tested in constant temperature oxidation furnace. The results showed that the oxidation weight gain of substrate was higher than that of coating, indicating that NiCrAlY coating played a protective role, the pinning phase can prevent crack propagation and improve the adhesion of the coating.

2. Experiment

The NiCrAlY coating was prepared by electrospark deposition. The substrate and the deposited material were NiCrAlY alloy. The main composition of the material was as shown in Table 1. The NiCrAlY alloy was quenched and tempered. The wire cutting method was used to process the substrate sample with a size of 20 mm × 10 mm × 3 mm and a Φ5 mm × 80 mm cylindrical electrode. Before deposition, the sample was polished with sandpaper and finally polished with emery gypsum with a particle size of 2.5 μm. Before high-temperature oxidation, all samples were ultrasonically cleaned with alcohol and deionized water. Coating deposition with SD-D5A spark deposition machine. The process is completed manually under argon protection. The deposition parameters are: power 1200 W, voltage 60 V, argon protection flow 20 L/min, alloy electrode specific deposition time 1.5 min/cm^2.

Place the intercepted substrate and the deposited sample in an oxidation crucible and conduct constant temperature oxidation test at 1000 ℃ in a muffle furnace. The weight change of the sample is measured by an electronic balance with a sensitivity of 0.1 mg. Weigh it every 20 h to observe the oxidation rate of the sample. Before weighing, take out the sample and cool it to room temperature in the air. The phase composition of the samples was analyzed by X-ray diffraction (XRD), and the morphology and element distribution of the samples were observed by scanning electron microscope (SEM/EDS).

Table 1. Composition of the NiCrAlY (wt%).

Elements	Ni	Cr	Al	Y
Composition	Bal.	27	11	0.5

3. Results

Fig. 1 is the morphology of NiCrAlY substrate and coating. As shown in Fig. 1(a), the coating surface forms a characteristic spatter-like morphology. When the electrode and the substrate contact in the form of short circuit, the capacitor energy is released instantaneously. A plasma arc current pulse with a maximum temperature of 5000-25000 K is generated in a very short time. At extremely high temperature, metal droplets form, and flow to the substrate surface at a high speed to form a splash morphology. Fig. 1(b) shows the cross-sectional morphology of the ESD coating. It can be seen from the Fig. 1(b) that the coating part is ultra-fine columnar grains. The unique deposition method of ESD makes the cooling rate during deposition reach 10^{-5}-10^{-6} ℃/s [11]. At the extremely fast cooling rate, the nucleated grains in the coating have no time to grow to form an ultra-fine columnar microcrystalline coating. It can be seen from Fig. 1(c) that is the morphology of the substrate alloy. The substrate structure is chrysanthemum-shaped, and there are a small number of pore defects.

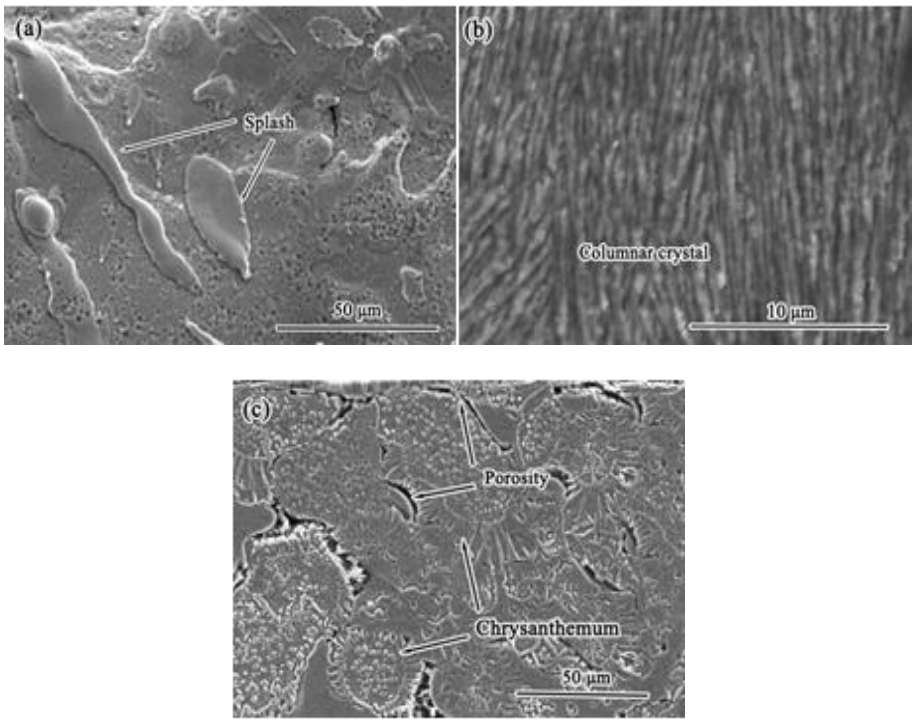

Fig. 1. Morphology of NiCrAlY substrate and coating deposited by ESD: (a) surface morphology of coating; (b) Cross-section morphology of coating; (c) Cross-section morphology of substrate.

The high-temperature oxidation kinetics curves of NiCrAlY alloy substrate and NiCrAlY coating are shown in Fig. 2. Both of the high-temperature oxidation kinetics curves follow the parabolic law. According to the formula:

$$y^2 = kt \tag{1}$$

where y is oxidation weight gain; T is the oxidation time, and Table 2 is the parabolic rate constant calculated according to formula (1). The calculation results are shown in Table 2. The parabolic rate constants of NiCrAlY alloy substrate are higher than those of NiCrAlY coating.

Fig. 2 is the oxidation kinetics curve of NiCrAlY alloy substrate and NiCrAlY coating in air at 1000 ℃ for 100 hours. The oxidation kinetics curves of NiCrAlY alloy substrate and NiCrAlY coating at high temperature follow the parabolic law, indicating that the high-temperature oxidation process of NiCrAlY alloy substrate and NiCrAlY coating conforms to the Wagner law. The diffusion and oxidation of elements are controlled by the oxide film [12]. From the high-temperature oxidation kinetics curve, it can be seen that the weight gain is fast before 40 h of high-temperature oxidation, and slow after 40 h, indicating that the oxide film formed on the alloy surface plays a role in protecting the internal metal of the alloy. It can be seen from Fig. 2 that the weight gain of the substrate after 100 h high-temperature oxidation is higher than that of the NiCrAlY coating, indicating that the NiCrAlY coating improves the high-temperature oxidation resistance of the substrate.

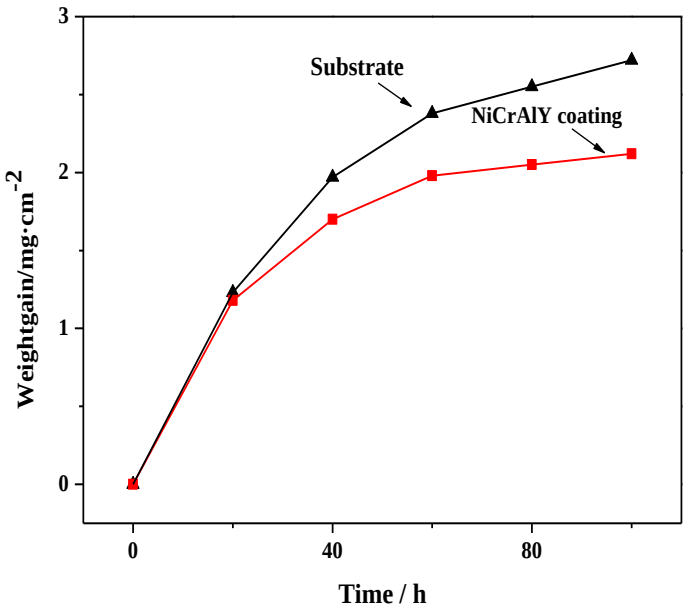

Fig. 2. High-temperature oxidation kinetic curves of NiCrAlY alloy substrate and NiCrAlY coating.

Table 2. Oxidation kinetics of NiCrAlY superalloy and NiCrAlY coating at 1000℃within respective time range.

Temperature (℃)	Sample	Oxidation duration (h)	k ($mg^2cm^{-4}s^{-1}$)	Oxidation duration (h)	k ($mg^2cm^{-4}s^{-1}$)
1000	Substrate	0-40	1.37×10^{-5}	40-100	3.36×10^{-6}
	Coating	0-40	1.18×10^{-5}	40-100	1.85×10^{-6}

Fig. 3 is the XRD spectrum of NiCrAlY alloy substrate and NiCrAlY coating oxidized in air at 1000 ℃ for 5 hours and 100 hours. It can be seen from the figure that the oxidation films of substrate and coating oxidized for 5 hours and 100 hours contain thermodynamic stable phases α-Al_2O_3, γ′-Ni3Al, α-Cr, Cr_2O_3, $NiCr_2O_4$ and NiO.

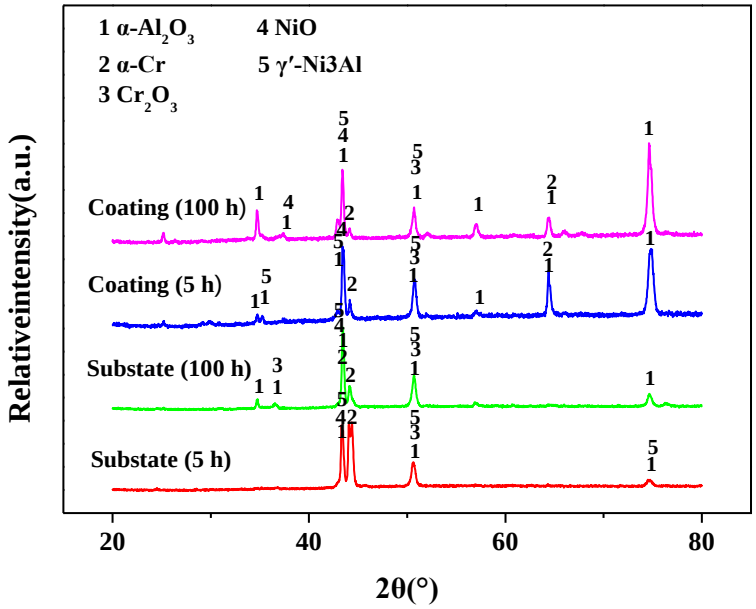

Fig. 3. XRD patterns of NiCrAlY alloy substrate and NiCrAlY coating after oxidation at 1000 °C for 5 h and 100 h.

Fig. 4. is the surface morphology of NiCrAlY alloy substrate and NiCrAlY coating oxidized at 1000 °C for 5 h and 100 h in air. Fig. 4(a), 4(b) is the surface morphology of substrate oxidized for 5 h and 100 h. Fig. 4(c), 4(d), 4(e) and 4(f) is the surface morphology of coating oxidized for 5 h and 100 h. It can be seen from Fig. 4(a) that a large amount of oxide film spalls off on the surface after high-temperature oxidation for 5 h. After the surface oxide film is peeled off, two regions are formed as shown in Fig. 4(a): the unpeeled zone 1 and the peeled zone 2. The XRD and EDS test results show that the main components of the 1 zone are α-Al_2O_3, and the main components of the 2 zone are NiO. The surface morphology of the substrate after oxidation for 100 h is shown in Fig. 4(b). It can be seen from the Fig. 4(b) that the oxide film on the substrate after oxidation for 100 h is seriously peeled off. XRD and EDS test results of the unpeeled zone 3 and the peeling zone 4 show that they are α-Al_2O_3. The above experimental phenomena show that

the Al_2O_3 film formed on the surface of the substrate after oxidation for 5 h has begun to peel off, and the peeling behavior of the oxide film continues until the end of the oxidation experiment. Fig. 4(c) and 4(d) show the surface morphology of NiCrAlY coating oxidized in air at 1000 °C for 5 h. It can be seen from Fig. 4(c) that after 5 h of coating oxidation, the surface of oxide film is flat and compact. Fig. 4(d) is obtained after enlarging Fig. 4(c). It can be seen from Fig. 4(d) that after 5 h of coating oxidation, a large number of flake oxygenates adhere to the surface, and there is no sign of oxide film peeling on the surface. XRD and EDS test results show that the main components of oxide film surface are α-Al_2O_3, Cr_2O_3. The surface morphology after oxidation for 100 h is shown in Fig. 4(e), and the oxide film remains flat and dense. Although there are a few debris on the surface of the coating after oxidation, there is no obvious peeling trace. The XRD and EDS test results show that the main components on the surface of the oxide film are α-Al_2O_3.

Table 3. EDS point results of oxide films of NiCrAlY superalloy and its coating.

Elements/at%	O	Al	Cr	Ni
1	53.73	38.78	2.81	4.58
2	41.68	4.57	11.33	42.42
3	46.19	38.16	3.87	11.78
4	49.18	45.55	1.58	3.69
5	35.03	38.21	20.94	5.63
6	57.49	40.04	0.78	1.69

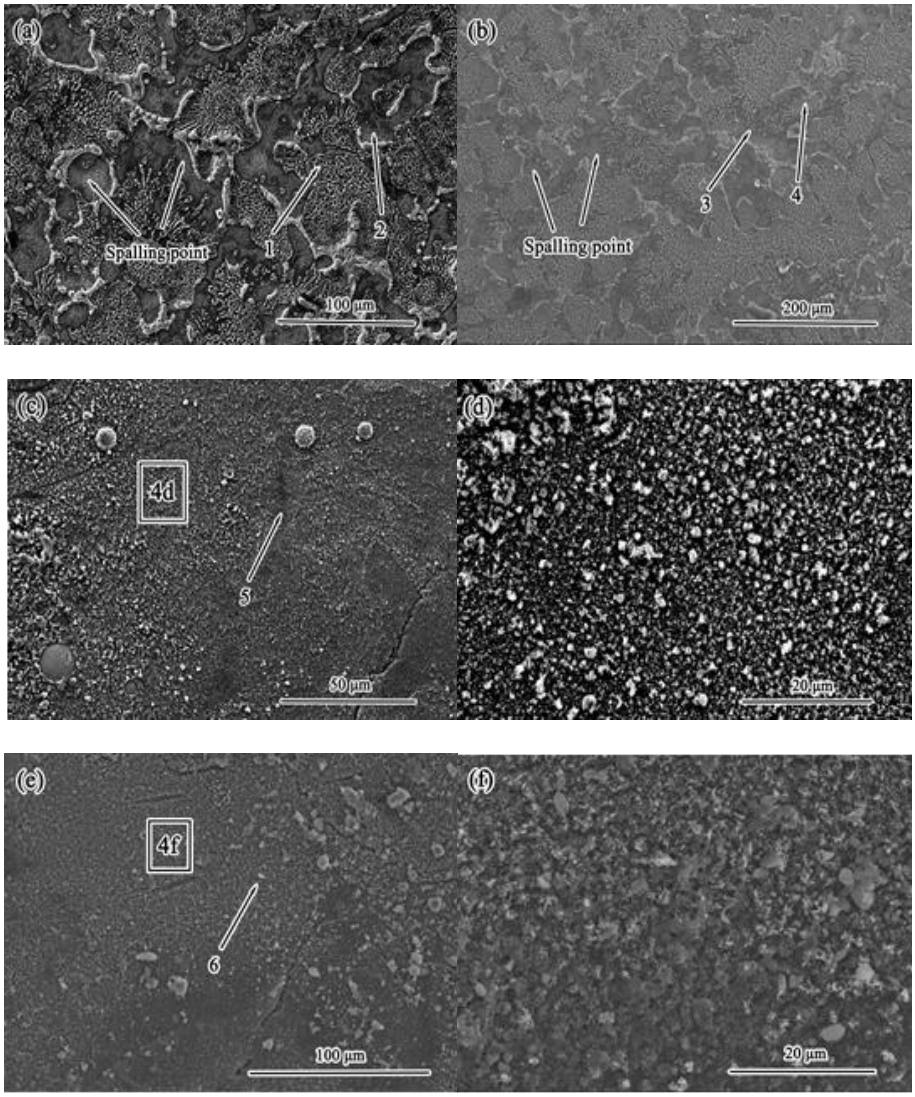

Fig. 4. The surface morphology of NiCrAlY alloy substrate and NiCrAlY coating after oxidation at 1000 °C: NiCrAlY alloy substrate oxidation 5 h (a) and oxidation 100 h (b); NiCrAlY coating oxidation 5 h (c), (d) and oxidation 100 h (e), (f).

Fig. 5 shows the cross-sectional morphology of NiCrAlY alloy substrate and NiCrAlY coating oxidized in air at 1000 ℃ for 5 h and 100 h. Fig. 5(a) and 5(b) show the cross-sectional morphology of the substrate after oxidation for 5 h and 100 h respectively. It can be seen from Fig. 5(a) that a layer of oxide film with thickness of about 0.5 μm has been formed on the surface of the substrate after oxidation for 5 h, and the thickness of the oxide film is thin and unevenly distributed. The EDS surface scanning analysis results show that the main component of the oxide film is Al_2O_3. After oxidation for 100 h, the oxide film is thickened and the thickness is about 2.5 μm. Fig. 5(c) and Fig. 5(d) are the cross-sectional morphologies of the coating after oxidation for 5 h and 100 h, respectively. It can be seen from Fig. 5(c) that a uniform and dense Al_2O_3 film is formed on the surface of the coating after oxidation for 5 h (Fig. 8). The thickness of the oxide film is about 1.5 μm. Compared with the surface oxide film of the substrate oxidized for 5 h, the thickness and density of the oxide film of the coating oxidized for 5 h are better than those of the

substrate oxide film. It is worth mentioning that the oxide film of the coating has shown a tendency to grow inside the substrate after oxidation for 5 h, so the adhesion of the oxide film of the coating is obviously better than that of the substrate. It can be seen from Fig. 5(d) that the NiCrAlY coating was oxidized at high temperature for 100 h to form a large number of pinned phases growing inside the substrate alloy. The pinned phase was partially cut into the substrate alloy. According to the EDS surface scanning results of the coating after oxidation (Fig. 9), the pinned phase was Al_2O_3, which played a role in enhancing the adhesion of the oxide film and formed the "pinning effect" [13].

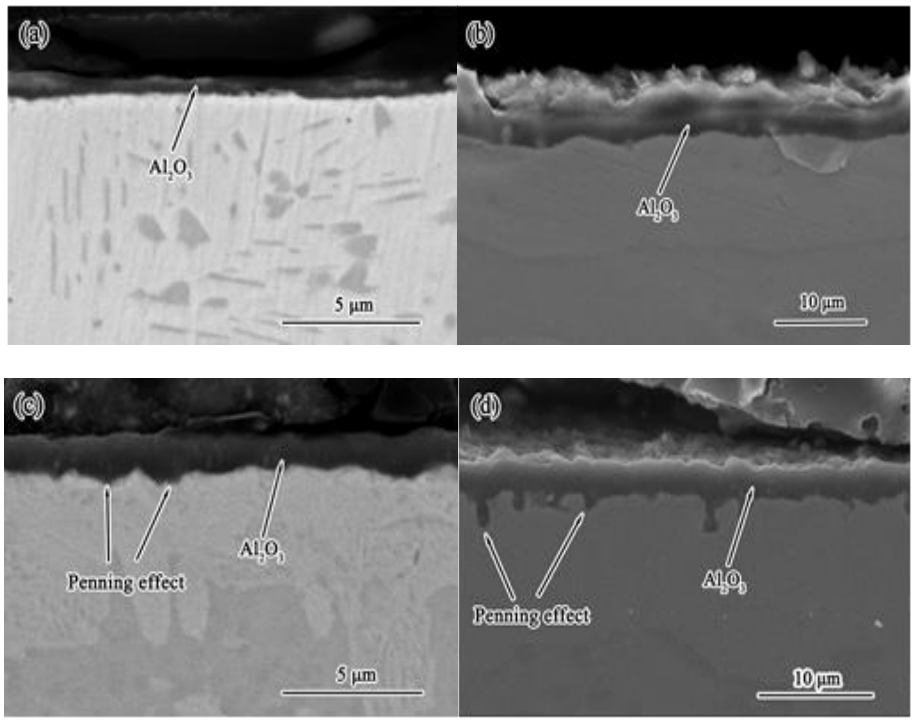

Fig. 5. Section morphology of NiCrAlY alloy substrate and NiCrAlY coating after oxidation at 1000 °C: NiCrAlY alloy substrate oxidation 5 h (a) and oxidation 100 h (b); NiCrAlY coating was oxidized for 5 h (c) and 100 h (d).

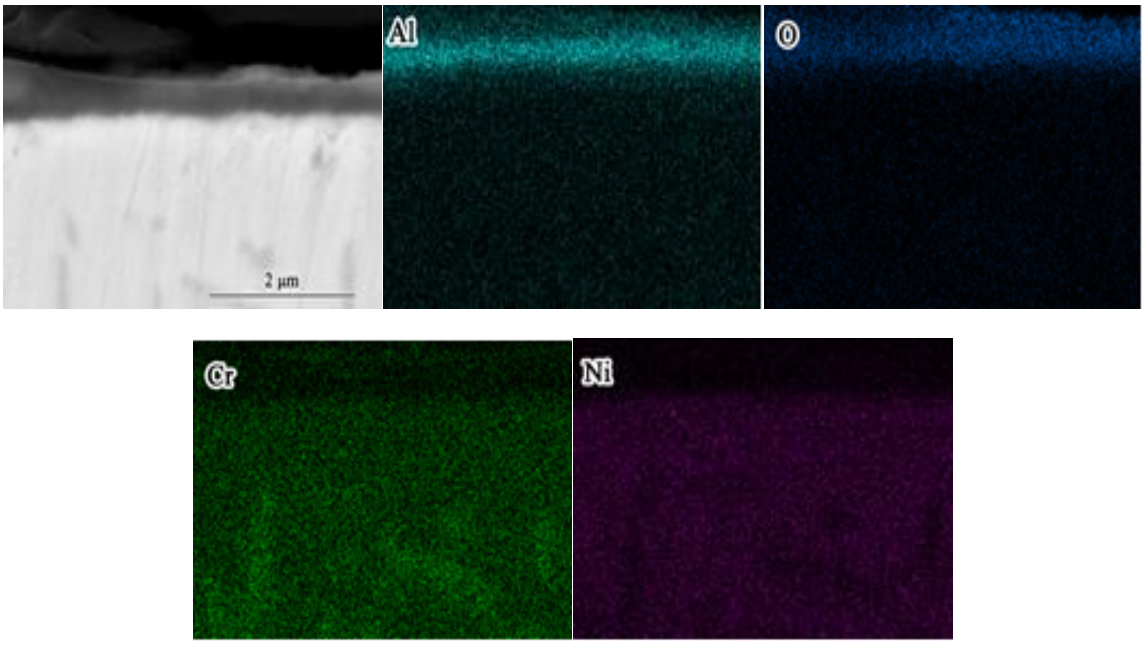

Fig. 6. EDS surface scanning results of NiCrAlY substrate oxidized at 1000 °C for 5 h.

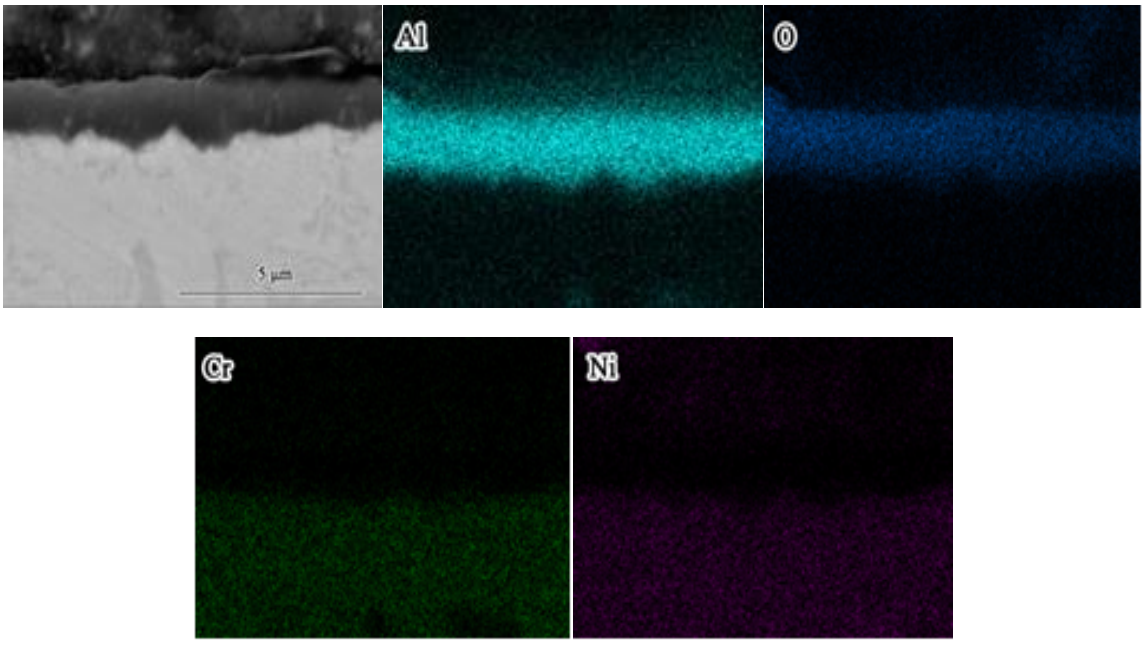

Fig. 7. EDS surface scanning results of NiCrAlY coating oxidized at 1000 °C for 5 h.

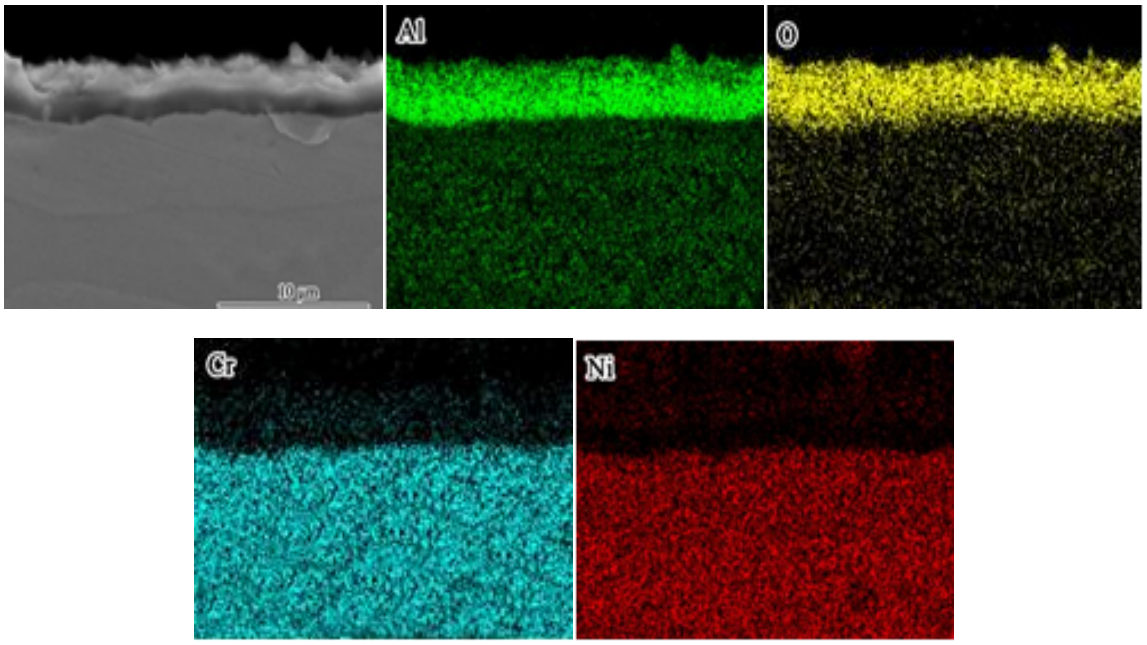

Fig. 8. EDS surface scanning results of NiCrAlY substrate oxidized at 1000 °C for 100 h.

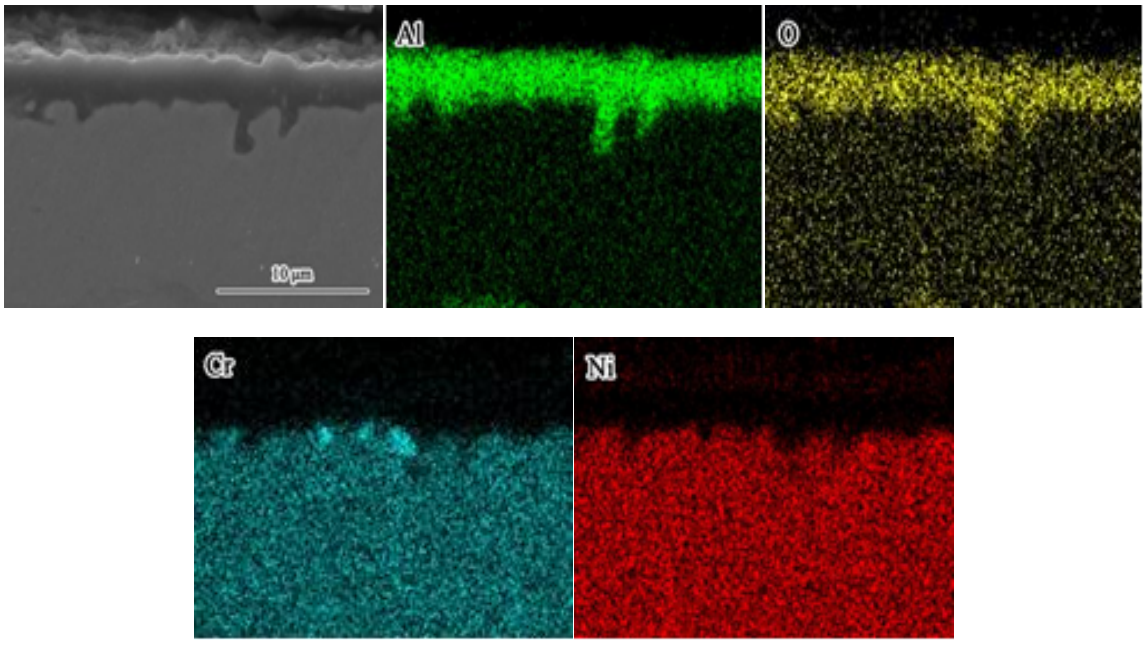

Fig. 9. EDS surface scanning results of NiCrAlY coating oxidized at 1000 °C for 5 h.

4. Discussions

The coating improves the oxidation resistance of the substrate mainly in two aspects. On the one hand, the weight gain of the oxidation kinetic curve of the coating is lower than that of the substrate, and on the other hand, the peeling resistance of the coating is significantly better than that of the substrate.

The weight gain of the oxidation kinetic curve of the coating is lower than that of the substrate: Wang et al.[10] reported that the smaller the grain size, the richer the grain boundary, and the faster the diffusion rate of Al element, thus reducing the critical concentration required for Al element from internal oxidation to external oxidation. Therefore, the formation of microcrystalline coating can accelerate the formation of Al_2O_3 film on the surface. After being oxidized for 5 hours, it can be seen from Fig. 5(a) and 5(c) that the thickness of the coating oxide film is significantly higher than that of the substrate. As a diffusion barrier layer, a thicker oxide film is more effective in preventing the diffusion of oxygen elements. To a certain extent, the oxidation weight gain of the coating is reduced. In addition, it was observed in the surface morphology of the substrate and the coating that the severe peel of the oxide film occurred in the high-temperature oxidation process of the substrate. The severe peel caused the internal alloy to lose the protective effect of the Al_2O_3 film, which undoubtedly increased the diffusion rate of oxygen elements attached to the oxide film surface to the inside, and accelerated the oxidation weight gain of the substrate.

Under normal circumstances, the oxide film undergoes plastic deformation under the action of stress, and there is stress in the oxide film. When the stress level is very high and the film is thin, the oxide film is prone to plastic deformation to release the stress. When the film/metal interface bond is strong, the oxide film will not peel off from the metal interface due to stress. There is generally compressive stress in the oxide film, equilibrium tensile stress exists in the metal, and shear stress exists in the oxide film/metal interface. In addition, there may be a tensile stress perpendicular to the metal surface in a local area of the oxide film. Under the above stress, the oxide film is prone to plastic deformation and forms an undulating morphology. Due to the unique deposition mode of ESD, the surface of the coating is rough and presents an uneven surface morphology. Therefore, the oxide film closely attached to the coating also fluctuates up and down. Under the action of the above two conditions, the oxide film grown is shown in Fig. 5(c) with obvious up-and-down morphology. When high-temperature oxidation is carried out, metal ions continue to diffuse outward from the inside of the metal under the driving force generated by the concentration gradient, and continue to form an oxide film in combination with the oxygen diffused inward from the outside. It can be seen from Fig. 10(a) and 10(b) that due to the unevenness of the oxide film/coating interface, at the convex to the coating (1, 2, 3), the diffusion path of metal ions in the columnar microcrystalline coating is shorter, while that in the oxide film is longer. In the concave to the substrate (4, 5) is the opposite, the diffusion path of metal ions in the columnar microcrystalline coating is longer, while the diffusion path in the oxide film is shorter. It is well known that the richer the grain boundary, the faster the diffusion rate of metal ions [14-15]. However, Al_2O_3 film as a diffusion barrier greatly slows down the diffusion rate of metal ions. In this paper, the NiCrAlY coating deposited by ESD has microcrystalline columnar crystal structure and rich grain boundaries. Therefore, the ion diffusion rate at the concave to the coating is higher than that at the convex to the substrate (Fig. 10b), and the metal ion diffusion flux per unit area at the concave to the coating is larger. Due to the rapid outward diffusion of metal

ions in the concave to the substrate, with the continuous high-temperature oxidation, a large amount of Al^{3+} in the concave to the substrate diffuses and migrates to the oxide film surface, resulting in the formation of pores at the oxide film/coating interface (Fig. 10c). At this time, due to the low oxygen partial pressure at the pores, the inward diffusion of adsorbed oxygen on the coating surface is accelerated, and finally oxygen reacts with Al^{3+} at the pores to form Al_2O_3. With the passage of oxidation time, the pores are gradually filled with Al_2O_3 and grow inward to form Al_2O_3 pinning phase as shown in Fig. 10(d).

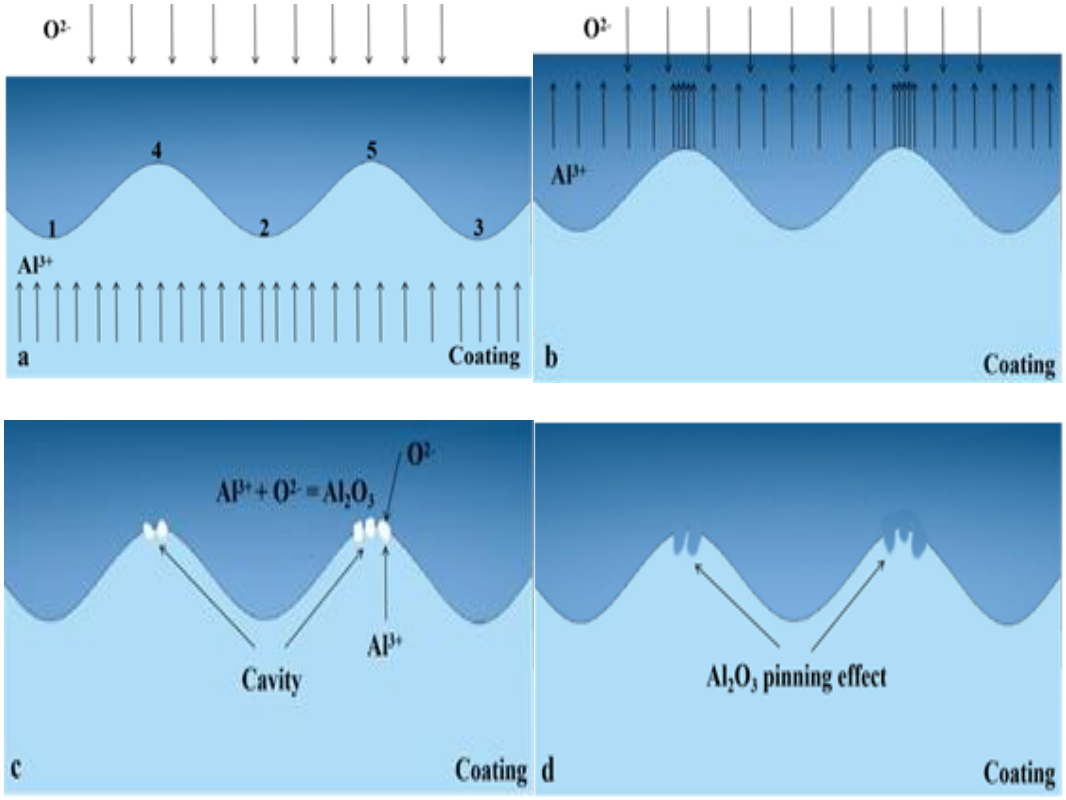

Fig. 10. Schematic diagram of "pinning effect".

It can be seen from Fig. 4 that a large area of oxide film peeling occurs after the oxidation of the substrate (Fig. 4a, 4b), while the oxide film remains intact after the oxidation of the coating (Fig. 4c, 4e). The above experimental facts show that the adhesion of the oxide film of the coating is strong. The main factors of strong coating adhesion can be summarized as follows: 1. In the process of high-temperature oxidation, the oxide is formed due to metal oxidation, and the volume of the oxide is different from that of the metal forming the oxide. According to the formula:

$$PBR = \frac{V_{oxi}}{V_m} \tag{2}$$

In formula (2), PBR value is pilling bedworth ratio, V_{oxi} is the volume of oxide, and V_m is the metal volume consumed to form oxide. It can be seen from previous studies, the PBR value of

α-Al_2O_3 is 1.28, which will lead to growth stress between oxide film and metal. Moreover, when new oxides grow in the formed oxide film, there will also be growth stress between the oxide film and the metal. When the temperature changes, thermal stress will be generated due to the difference of linear expansion coefficient between oxide film and metal. When the internal stress of the oxide film is high enough and the oxide film cannot release the stress through deformation, the film will produce fine cracks under the action of stress. As the oxidation goes on, the cracks penetrate the oxide film and cause the film to peel off.

According to the formula:

$$\sigma = \left(\frac{E^* G_c}{\pi c} \right)^{\frac{1}{2}} \tag{3}$$

In Formula (3), c is the length, σ is the tensile stress required to increase the crack growth of a length of C, E^* is the effective Young's modulus of the film-metal system, and G_c is the critical crack growth force. Studies have shown that the existence of pinned phase can effectively prevent the crack propagation [13, 16]. In the oxide film with pinned phase, if you want to add a crack with length c, the critical propagation force needs to be increased. This is also confirmed in Fig. 4. The surface morphology Fig. 4(b) of the substrate oxidized for 100 h shows that the oxide film on the substrate surface is seriously peeled off, and the peeling points are all over the surface of the substrate alloy. The surface morphology Fig. 4(e) of the coating oxidized for 100 h shows that the oxide film on the coating surface remains flat and compact after high-temperature oxidation, and there is no peeling point, indicating that the stress required for the peeling of the coating oxide film is high, so its adhesion is obviously better than that of the substrate alloy oxide film. Becher et al. [17] studies on metal-glass interface also show that fracture energy reaches its maximum when macroscopic mechanical interlocking interface is formed between metal and glass layer. The pinning phase increases the contact area between the oxide film and the metal, thus enhancing the bonding strength of the interface, improving the adhesion of the oxide film by preventing the diffusion of cracks, reducing the possibility of the peeling off of the oxide film, and forming an obvious “pinning effect” [13]. 2. Formation of microcrystalline coating: The spallation of oxide film is usually caused by thermal stress and growth stress. Thermal stress and growth stress usually exist in the process of high temperature oxidation. The oxide film peels off under stress, exposing the metal inside the alloy, and accelerating the internal oxidation of the alloy. Geng et al. [15] found that the oxide film formed by microcrystalline coating has smaller grain size and better deformation ability, which is conducive to releasing growth stress and thermal stress through plastic deformation. Therefore, it has good adhesion and the oxide film is not easy to peel off. It can be seen from Fig. 1(b) that the NiCrAlY coating deposited by ESD in this paper is a columnar microcrystalline coating. The coating oxide film releases the stress well in the process of high-temperature oxidation and effectively improves the adhesion of the coating oxide film. The above research shows that the microcrystalline columnar crystal structure deposited by ESD is beneficial to the formation of the pinning phase in the oxide film, which can effectively improve the adhesion of the oxide film and improve the oxidation resistance of the coating. To a certain extent, this research provides a theoretical basis for the oriented preparation of coatings with high-quality anti-stripping performance.

5. Conclusions

1 There is a short-range diffusion path of metal ions in the columnar microcrystalline coating deposited by ESD. The existence of the short-range diffusion path is conducive to the rapid migration of metal ions in the coating. Smaller pores nucleate and gradually grow where the metal ion diffusion flux is large. The inward diffused oxygen at the pores reacts with the outward diffused metal Al^{3+} elements, and finally forms a pinning phase at the film/coating interface that can significantly enhance the anti peeling performance of the film.

2 The existence of pinning phase can effectively prevent the crack propagation caused by the internal stress of the film, improve the critical tensile stress required for crack propagation, reduce the possibility of penetrating crack and improve the adhesion of oxide film.

3 The columnar microcrystalline coating deposited by ESD has better adhesion because the oxide film has smaller grain size and better deformation ability, which is conducive to releasing growth stress and thermal stress through plastic deformation.

Acknowledgments

The authors are grateful for the financial support of the National Science Foundation of Liaoning Province of China (No.20180550353, 2019-ZD-0264), and the Supporting Project of Middle-young Aged Innovative Talents of Science and Technology of Shenyang City (RC190292), and the Supporting Project of Innovative Talents of Colleges and Universities of Liaoning Province (LR2019059), and the Research Innovation Team Building Program of Shenyang Ligong University, and basic scientific research project of Liaoning Provincial Department of Education (LJKZ0274).

References

[1] L. D. Zhao, M. Parco, E. Lugscheider, Surface & Coatings Technology 184, 298 (2004); https://doi.org/10.1016/j.surfcoat.2003.10.055

[2] A. Bonadei, T. Marrocco, Surface & Coatings Technology 242, 200 (2014); https://doi.org/10.1016/j.surfcoat.2013.08.019

[3] F. Ghadami, A. R. Aghdam, A. Zakeri et al., Ceramics International 46(4), 4556 (2020); https://doi.org/10.1016/j.ceramint.2019.10.184

[4] H. Chen, A. Rushworth, X. Hou et al., Surface and Coatings Technology 363, 400 (2019); https://doi.org/10.1016/j.surfcoat.2019.02.024

[5] Y. Zhang, Journal of metals 67, 2599 (2015); https://doi.org/10.1007/s11837-015-1640-0

[6] E. Hejrani, D. Sebold, W. J. Nowak et al., Surface and Coatings Technology 313, 191 (2017); https://doi.org/10.1016/j.surfcoat.2017.01.081

[7] J. L. Wang, M. H. Chen, S. L. Zhu et al., Applied Surface Science 345, 194 (2015); https://doi.org/10.1016/j.apsusc.2015.03.157

[8] L. D. Zhao, M. Parco, E. Lugscheider, Surface & Coatings Technology 184(2-3), 298 (2004);

https://doi.org/10.1016/j.surfcoat.2003.10.055

[9] J. M. Tang, Applied Surface Science 365, 202 (2016); https://doi.org/10.1016/j.apsusc.2015.12.198

[10] J. L. Wang, M. H. Chen, S. L. Zhu, F. H. Wang, Applied Surface Science 345, 194 (2015); https://doi.org/10.1016/j.apsusc.2015.03.157

[11] C. A. Guo, T. Liang, F. S. Lu, Z. G. Liang, S. Zhao, J. Zhang, Materiali in Tehnologije 53(3), 389 (2019); https://doi.org/10.17222/mit.2018.210

[12] T. J. Nijdam, W. G. Sloof, Oxidation of Metals 69(1-2), 1 (2008); https://doi.org/10.1007/s11085-007-9080-z

[13] X. R. Ren, H. L. Shi, W. H. Wang et al., Journal of the European Ceramic Society 40(2), 203 (2020); https://doi.org/10.1016/j.jeurceramsoc.2019.10.006

[14] Y. Ping, W. Wen, F. H. Wang et al, Surface & Coatings Technology 206(1), 68 (2011); https://doi.org/10.1016/j.surfcoat.2011.06.037

[15] S. J. Geng, F. H. Wang et al., Oxidation of Metals 57, 231 (2002); https://doi.org/10.1023/A:1014870101143

[16] M. S. Li, High temperature corrosion of metals, Beijing, Metallurgical Industry Press, 118 (2001).

[17] P. F. Becher, W. L. Newell, Journal of Materials Science 12(1), 90 (1977); https://doi.org/10.1007/BF00738474